Molecular Crystals and Liquid Crystals

Publication details, including instructions for authors and subscription information:
http://www.tandfonline.com/loi/gmcl20

Director Dynamics Within a Boundary Layer in Contact with a Shearing Solid Surface With Non-Rigid Anchoring

Alain R. Véron [a] & Assis F. Martins [a]

[a] Dpt. Ciência dos Materiais and I3N/CENIMAT, Faculdade de Ciências e Tecnologia, Universidade Nova de Lisboa, Caparica, Portugal

Version of record first published: 30 Jan 2009

To cite this article: Alain R. Véron & Assis F. Martins (2008): Director Dynamics Within a Boundary Layer in Contact with a Shearing Solid Surface With Non-Rigid Anchoring, Molecular Crystals and Liquid Crystals, 495:1, 294/[646]-311/[663]

To link to this article: http://dx.doi.org/10.1080/15421400802430380

Mol. Cryst. Liq. Cryst., Vol. 495, pp. 294/[646]–311/[663], 2008

ISSN: 1542-1406 print/1563-5287 online
DOI: 10.1080/15421400802430380

Taylor & Francis
Taylor & Francis Group

Director Dynamics Within a Boundary Layer in Contact with a Shearing Solid Surface With Non-Rigid Anchoring

Alain R. Véron and Assis F. Martins
Dpt. Ciência dos Materiais and I3N/CENIMAT, Faculdade de Ciências e Tecnologia, Universidade Nova de Lisboa, Caparica, Portugal

The hydrodynamics of liquid crystals within thin boundary layers in contact with solid surfaces is strongly perturbed by the director anchoring on these surfaces; that manifests by occurrence of strong gradients and backflows. Accordingly, it is legitimate to question the interpretation of rheological measurements based on flow properties in the bulk where, moreover, director and velocity gradients are often assumed to be homogeneous. This remark is enhanced by the fact that rheology probes the fluid in contact with a solid surface. On the other hand, comparison between theoretical predictions and experimental observations close to the solid surface may shed light on the nematic-solid interaction. For these reasons the director dynamics at a solid surface deserves to be analysed theoretically. We have investigated the effect of non-rigid anchoring within the frame-work of Leslie-Ericksen theory combined with Rapini-Papoular model [A. Rapini, M. Papoular, J. Phys., 30C, 4, (1969)] for which the surface energy density is characterised by an anchoring strength and a preferred orientation of the director called easy axis. Calculations have been performed for nematics enclosed between two parallel plates in relative motion. Results for aligning and tumbling low molecular weight liquid crystals are presented. They may be summarised as follows: (i) strong inhomogeneities close to the surfaces, (ii) director precession at the surface for aligning nematics under certain conditions and (iii) relaxation of the stored elastic energy for tumbling nematics.

Keywords: boundary layer; Leslie-Ericksen; nematic; shear; tumbling; weak anchoring

This work was partly supported by the "Fundação para a Ciência e a Tecnologia" (Portugal) under research grant SFRH/BPD/8894/2002 to A. Véron.

Address correspondence to Assis F. Martins, Dpt. Ciência Dos Materiais and CENIMAT, Faculdade de Ciências e Technologia, Universidade Nova de Lisboa, 2829-516 Caparica, Portugal. E-mail: asfm@fct.unl.pt

I. INTRODUCTION

The hydrodynamics of nematic liquid crystals is described by the well-known Leslie-Ericksen theory that couples the director to the flow velocity [1,2]. However, in practice this theory must be completed by taking into account the interaction between the liquid crystal and the solid surfaces that enclose the fluid. Indeed, director anchoring on the solid surface induces strong perturbations of the fluid state within (at least) a thin boundary layer. Such perturbations may have important effects, for example in rheological measurements, since the currently used techniques probe the force exerted by the fluid in contact with the surface on which the measurement is performed. The Leslie-Ericksen theory is well established experimentally, but models describing the director-solid surface interaction are less well known. Theoretical studies of nematodynamics in the vicinity of a shearing surface may shed light on this topic.

In this work we analyse the director dynamics in the vicinity of a shearing solid surface for the simple infinite parallel plate geometry. The interaction between the director and the solid surface is described with the Rapini-Papoular model [3]. We evidence two different features occurring within the boundary layer in contact with the plates; one is obtained with aligning nematics, the other one with tumbling nematics.

II. THEORY

II-1 Generalities and Basic Assumptions

In this section the general Leslie-Ericksen theory is restricted to situations where the three following assumptions can safely be made: (i) the one-constant approximation, i.e., the three Frank elastic constants are assumed to be equal, (ii) negligible inertia and (iii) negligible convective contribution, i.e., $d/dt \approx \partial/\partial t$. Under theses hypotheses the extra stress tensor τ reads

$$\tau_{ij} = L_{ijpq} V_{p,q} + S_{ij} \quad (i,j,p,q = 1,2,3) \tag{1}$$

with

$$L_{ijpq} = \frac{1}{2} \left\{ \begin{array}{c} 2\alpha_1 n_i n_j n_p n_q + \alpha_4(\delta_{ip}\delta_{jq} + \delta_{iq}\delta_{jp}) \\ +(\alpha_5 + \alpha_2) n_i n_p \delta_{jq} + (\alpha_5 - \alpha_2) n_i n_q \delta_{jp} \\ +(\alpha_6 + \alpha_3) n_j n_p \delta_{iq} + (\alpha_6 - \alpha_3) n_j n_q \delta_{ip} \end{array} \right\} \tag{2}$$

and

$$S_{ij} = \alpha_2 n_i \frac{\partial n_j}{\partial t} + \alpha_3 n_j \frac{\partial n_i}{\partial t} - K n_{k,i} n_{k,j} \tag{3}$$

In Eqs. (1) to (3) $V_p (p = 1, 2, 3)$ denotes the pth component of the velocity, $\alpha_i (i = 1, \ldots, 6)$ the Leslie viscosities,[1] $n_i (i = 1, 2, 3)$ the ith component of the director and K the single Frank elastic constant. On the other hand, the two equations of motion of Leslie-Ericksen theory reduce to

$$-\frac{\partial p}{\partial x_i} + \frac{\partial \tau_{ji}}{\partial x_j} = 0 \quad i,j = 1,2,3 \tag{4}$$

and

$$\gamma_1 \frac{\partial n_i}{\partial t} = -\alpha_2 n_j V_{i,j} - \alpha_3 n_j V_{j,i} + K n_{i,jj} + \lambda n_i \quad (i,j = 1,2,3) \tag{5}$$

where p denotes the pressure, $\gamma_1 = \alpha_3 - \alpha_2$ and λ is a Lagrange multiplier associated with the condition $\vec{n} \cdot \vec{n} = 1$.

II-2. Parallel Plates Geometry

We consider the flow of a nematic liquid crystal enclosed between two parallel infinite plates a distance d apart, one of these plates being in motion with a velocity constant in magnitude and in direction. The equations of motion are written in the following system of Cartesian axes: the x_1 axis is chosen parallel to the velocity of the moving plate, the x_2 axis is normal to the plates and the x_3 axis is along the vorticity. Moreover we consider that the inhomogeneities are only along the direction normal to the plates (i.e., the x_2 axis), which is expected because of director anchoring. Under these assumptions three velocity gradients arise, namely, $V_{1,2}$, $V_{2,2}$, and $V_{3,2}$, but the incompressibility condition entrains $V_{2,2} = 0$ and finally $V_2 = 0$ because the component of the velocity normal to the bounding plates vanishes on these plates. Accordingly, the system of equations given by Eq. (4) may be reduced to

$$\begin{cases} \dfrac{\partial \tau_{21}}{\partial x_2} = 0 & \text{(a)} \\ \dfrac{\partial \tau_{23}}{\partial x_2} = 0 & \text{(b)} \end{cases} \tag{6}$$

for the two unknowns V_1 and V_3 (for a given director profile). With $\tau_{21} = L_{2112} V_{1,2} + L_{2132} V_{3,2} + S_{21}$ and $\tau_{23} = L_{2312} V_{1,2} + L_{2332} V_{3,2} + S_{23}$, which results from Eq. (1) applied to the current flow model, Eq. (6) may be expanded as follows[2]

[1]The Leslie viscosities satisfy the Parodi relation $\alpha_2 + \alpha_3 = \alpha_6 - \alpha_5$.
[2]Note that the elastic contribution vanishes in S_{21} and S_{23}.

$$\begin{cases} L_{2112,2}V_{1,2} + L_{2132,2}V_{3,2} + L_{2112}V_{1,22} + L_{2132}V_{3,22} + S_{21,2} = 0 \\ L_{2312,2}V_{1,2} + L_{2332,2}V_{3,2} + L_{2312}V_{1,22} + L_{2332}V_{3,22} + S_{23,2} = 0 \end{cases} \tag{7}$$

On the other hand, within the current model the general director equation, i.e., Eq. (5), reduces to

$$\begin{cases} \gamma_1 \dfrac{\partial n_1}{\partial t} = -\alpha_2 n_2 V_{1,2} + K n_{1,22} + \lambda n_1 \\ \gamma_1 \dfrac{\partial n_2}{\partial t} = -\alpha_3 n_1 V_{1,2} - \alpha_3 n_3 V_{3,2} + K n_{2,22} + \lambda n_2 \\ \gamma_1 \dfrac{\partial n_3}{\partial t} = -\alpha_2 n_2 V_{3,2} + K n_{3,22} + \lambda n_3 \end{cases} \tag{8}$$

This latter system of equations is solved with non-rigid boundary conditions for the director. It means that the director on the plates can move away from a particular direction $\vec{e}$, called easy axis, with a finite energy cost related to the anchoring strength A_s. When a Rapini-Papoular like surface energy [3] is added to the volume energy associated with Frank elasticity [2], the static director configuration that minimises the total energy satisfies the boundary conditions [4]

$$K u_j n_{i,j} = h_{si}^{\perp} \quad i,j = 1,2,3 \tag{9}$$

where $\vec{u}$ denotes the outward unit vector normal to the boundary and $\vec{h}_s^{\perp}$ is defined by

$$\vec{h}_s^{\perp} = A_s(\vec{e}\cdot\vec{n})\vec{e}^{\perp} \tag{10}$$

with

$$\vec{e}^{\perp} = \vec{e} - (\vec{e}\cdot\vec{n})\vec{n} \tag{11}$$

The condition given by Eq. (9), rigorous for static problems, is assumed to be still valid in dynamics. For plates normal to the x_2 axis we have $u_1 = 0$, $u_2 = \pm 1$ and $u_3 = 0$; accordingly Eq. (9) yields

$$K\frac{\partial \vec{n}}{\partial n_2} = u_2 \vec{h}_s^{\perp} \tag{12}$$

When the director is constrained to stay within the shear plane (i.e., $n_3 = 0$) Eqs. (7) and (8) reduce to

$$\begin{cases} L_{2112,2}V_{1,2} + L_{2112}V_{1,22} + S_{21,2} = 0 & \text{(a)} \\ L_{2332,2}V_{3,2} + L_{2332}V_{3,22} = 0 & \text{(b)} \end{cases} \tag{13}$$

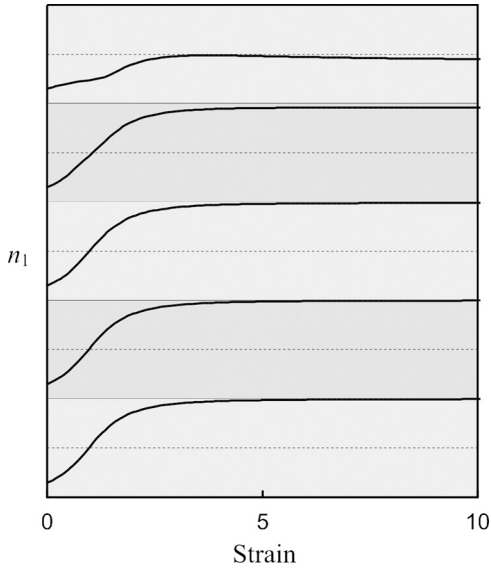

FIGURE 1 Strain dependence of the component n_1 of the director for $\dot{\gamma} = 4s^{-1}$ and for different positions: from the top to the bottom we have $x_2/d = 1.00$, $x_2/d = 0.96$, $x_2/d = 0.93$, $x_2/d = 0.90$ and $x_2/d = 0.70$. These results have been obtained by solving Eqs. (7) and (8) with data of Tables 1 and 2. In this case there is no oscillation at all.

and

$$\begin{cases} \gamma_1 \dfrac{\partial n_1}{\partial t} = -\alpha_2 n_2 V_{1,2} + K n_{1,22} + \lambda n_1 \\ \gamma_1 \dfrac{\partial n_2}{\partial t} = -\alpha_3 n_1 V_{1,2} + K n_{2,22} + \lambda n_2 \end{cases} \tag{14}$$

We note that Eq. (13b) combined with the non-slippage condition for the velocity implies $V_3 = 0$ everywhere so that Eqs. (13a) and (14) constitute a closed system of equations when the director stays within the shear plane.

The continuous equations for the director and the velocity are discretised and solved numerically. For both equations a centered finite difference scheme is used for spatial derivatives. The discretisation of Eqs. (7) or (13a) lead to a system of linear equations with respect to velocity characterised by a tridiagonal matrix, wich is efficiently solved by employing the Thomas algorithm [5]. On the other hand the discretisation of spatial derivatives in Eqs. (8) or (14) yields a set

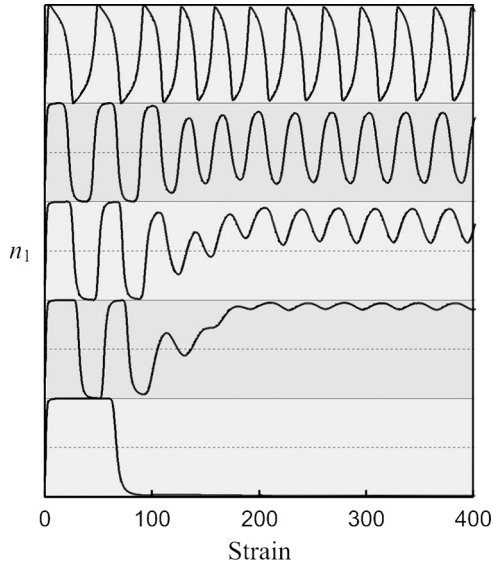

FIGURE 2 Strain dependence of the component n_1 of the director for $\dot{\gamma} = 15s^{-1}$ and for different positions: from the top to the bottom we have $x_2/d = 1.00$, $x_2/d = 0.96$, $x_2/d = 0.93$, $x_2/d = 0.90$ and $x_2/d = 0.70$. These results have been obtained by solving Eqs. (7) and (8) with data of Tables 1 and 2. Oscillations occur in the vicinity of the plates ($x_2/d = 1.00$) but not in the bulk ($x_2/d = 0.70$).

of differential equations with respect to time derivative that is solved with the Runge-Kutta method.

III. RESULTS AND DISCUSSION

For numerical applications the orientation of the easy axis $\vec{e}$ is specified by the angles β_e and ψ_e as follows

$$\begin{cases} e_1 = \cos\psi_e \sin\beta_e \\ e_2 = \sin\psi_e \sin\beta_e \\ e_3 = \cos\beta_e \end{cases} \tag{15}$$

and the anchoring strength A_s used in this work is consistent with experimental data [6]. We now precise the conventions used for the graphical representation of space or strain dependence of the director (that concerns Figs. 1 to 9). Each curve representing one director component lies within a gray rectangular band, for clarity

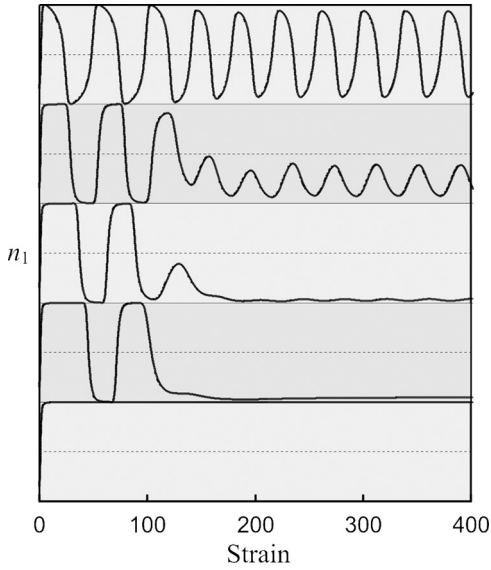

FIGURE 3 Strain dependence of the component n_1 of the director for $\dot{\gamma} = 40s^{-1}$ and for different positions: from the top to the bottom we have $x_2/d = 1.00$, $x_2/d = 0.96$, $x_2/d = 0.93$, $x_2/d = 0.90$, $x_2/d = 0.70$. These results have been obtained by solving Eqs. (7) and (8) with data of Tables 1 and 2. Oscillations occur in the vicinity of the plates ($x_2/d = 1.00$) but not in the bulk ($x_2/d = 0.90$, $x_2/d = 0.70$).

two gray-levels are used to clearly separate two consecutive bands within the same figure. The broken horizontal line in the middle of each band defines the zero of the director component plotted within this band while the upper and lower limits of each band correspond to the extreme values -1 and $+1$ of this director component.

III-1 Aligning Nematics

In this subsection the model described in Section II is applied to the aligning system MBBA at 20°C. The model parameters (i.e., β_e, ψ_e, d, A_s) are given in Table 1 while the material parameters (i.e., $\alpha_1, \ldots, \alpha_6$ and K) are given in Table 2. The viscosities come from [7] while the magnitude of the single elastic constant is estimated from the data for 5CB [8]. The easy axis defined in Table 1 is neither homeotropic ($\beta_e = \pi/2,\ \psi_e = \pi/2$) nor planar ($\psi_e = 0$). It actually lies close to the shear plane by making with the normal to the plate an angle of about 45°; the reason for this choice will appear later.

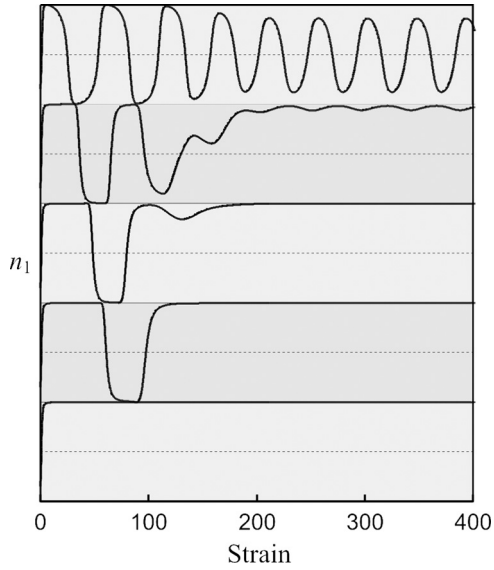

FIGURE 4 Strain dependence of the component n_1 of the director for $\dot{\gamma} = 80s^{-1}$ and for different positions: from the top to the bottom we have $x_2/d = 1.00$, $x_2/d = 0.96$, $x_2/d = 0.93$, $x_2/d = 0.90$ and $x_2/d = 0.70$. These results obtained by solving Eqs. (7) and (8) with data of Tables 1 and 2. Oscillations occur in the vicinity of the plates ($x_2/d = 1.00$) but not in the bulk ($x_2/d = 0.93$, $x_2/d = 0.90$, $x_2/d = 0.70$).

Figures 1 to 4 show the strain (or time) dependence of the component n_1 of the director for several shear rates. Each figure contains several director responses corresponding to different positions between the plates, namely, for x_2/d equal to 1, 0.96, 0.93, 0.9, and 0.7.[3] The main result is the occurrence of an oscillatory regime characterised by director precession on the plates and in the vicinity of the plates (see Fig. 2 for $x_2/d \geq 0.9$; Fig. 3 for $x_2/d \geq 0.93$; Fig. 4 for $x_2/d \geq 0.96$) while a steady solution is rapidly reached in the bulk (see Fig. 2 for $x_2/d \leq 0.7$; Fig. 3 for $x_2/d \leq 0.9$; Fig. 4 for $x_2/d \leq 0.93$). This description is confirmed by Figure 5 that shows some profiles of n_1 at different strains (or times) for $\dot{\gamma} = 15s^{-1}$ after a delay corresponding to about five full rotations of the director on the plates. Indeed, one may observe that the director varies in time only close to the bounding plates (see the boundary layers delimited by the vertical dotted lines) while it aligns close to the velocity in the bulk (i.e., $n_1 \approx \pm 1$ between

[3]The profiles being symmetric with respect to the middle gap at each time (see Fig. 5) the behaviour shown by Figures 1–4 close to $x_2 = 0$ arise also close to $x_2 = d$.

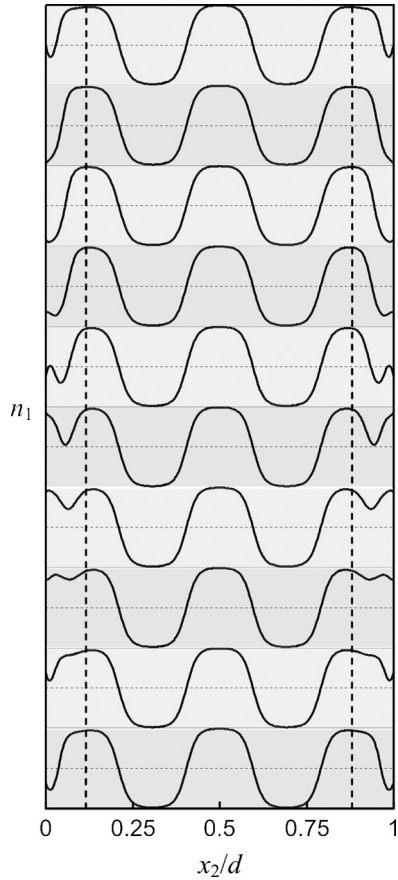

FIGURE 5 Profiles of n_1 for MBBA at different strains γ_i: from the top to the bottom we have $\gamma_i = \gamma_0 + i\gamma_1$ with $\gamma_0 = 205$, $\gamma_1 = 3.99$ and $i \approx 0,\ 1, \ldots, 9$. The value of $9 \times \gamma_1$ corresponds approximately to a rotation by 2π of the director on the plates. These results have been obtained by solving Eqs. (7) and (8) with data of Tables 1 and 2. Between the two vertical dotted lines the director is stationary; on the contrary in the vicinity of the boundaries the director is time dependent.

the vertical dotted lines). It should be noted that this local oscillatory regime is not general, it depends on the parameters; thus for $\dot{\gamma} = 4s^{-1}$ no oscillations occur, as shown in Figure 1. In other words, the space of parameters may be separated in (at least) two domains, one where the system reaches a steady solution everywhere and another one where a permanent precession regime arises within boundary layers.

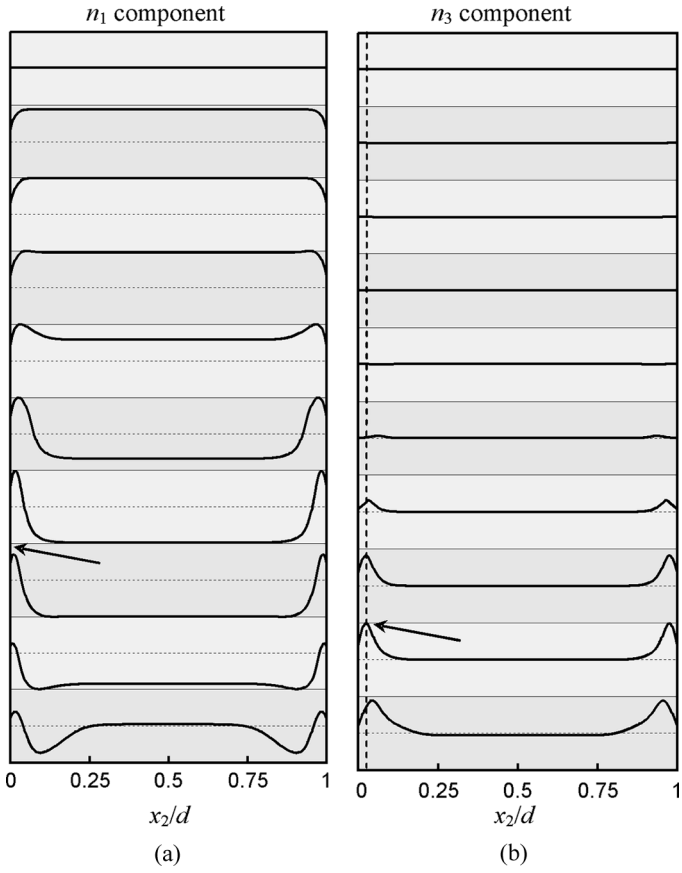

FIGURE 6 Director profiles for 8CB at different strains γ_i: from the top to the bottom we have $\gamma_i = i\gamma_0$ with $\gamma_0 = 1.87$ and $i \approx 0, 1, \ldots, 9$. Component n_1 in (a) and component n_3 in (b). The value of $9 \times \gamma_0$ corresponds approximately to a rotation by 2π of the director within the shear plane. These results have been obtained by solving Eqs. (7) and (8) with data of Tables 3 and 4. The dotted vertical line materialises the abscissa x_2^* defined in the text. The formation of the peaks for n_3 coincides with the unhook of n_1 from $+1$ as indicated by the arrows.

The following general features emerge concerning the shear stress response of aligning nematics. There is no oscillatory regime for rigid anchoring, so that our finding appears specific to non-rigid anchoring. The amplitude of the precession is maximum on the bounding plates, it decreases rapidly with increase of the distance to the plate and the director becomes stationary in the bulk (see Figs. 2 to 5). The depth of the boundary layer where the precession amplitude is notable

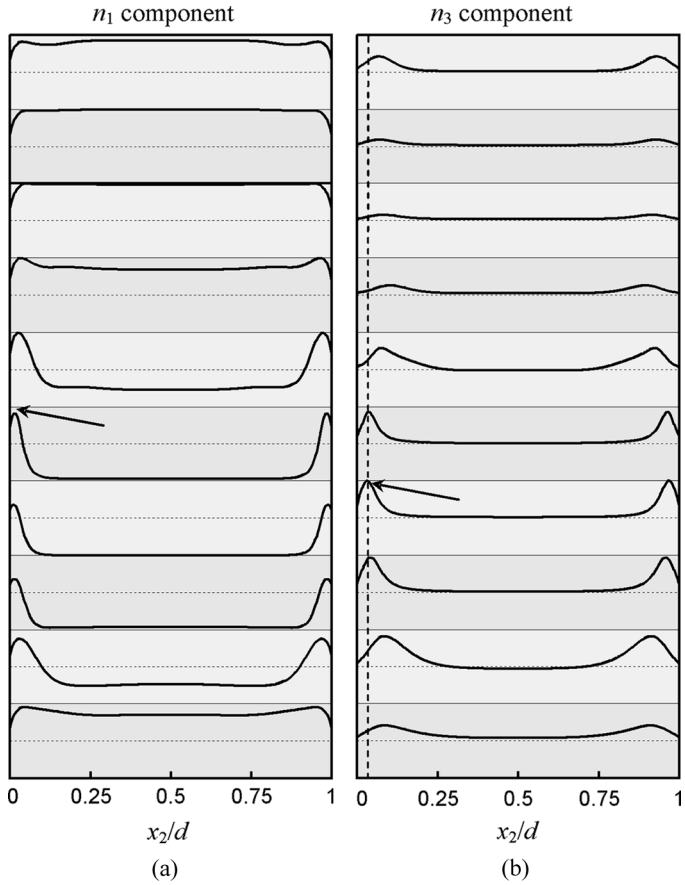

FIGURE 7 Director profiles for 8CB at different strains γ_i: $\gamma_i = i\gamma_0$ with $\gamma_0 = 1.87$ and $i \approx 10, 11, \ldots, 19$. Component n_1 in (a) and component n_3 in (b). The value of $9 \times \gamma_0$ corresponds approximately to a rotation by 2π of the director within the shear plane. These results have been obtained by solving Eqs. (7) and (8) with data of Tables 3 and 4. The dotted vertical line materialises the abscissa x_2^* defined in the text. The formation of the peaks for n_3 coincides with the unhook of n_1 from $+1$ as indicated by the arrows.

amounts to about 30 μm. In the bulk the director aligns with a direction close to the velocity as expected (see Fig. 5). It should however be noted that director and velocity do not necessarily point in the same or opposite direction everywhere so that inversion walls in which the director abruptly rotates by about π may arise in the bulk as shown in Figure 5. Actually, these walls are created in the vicinity of the plates

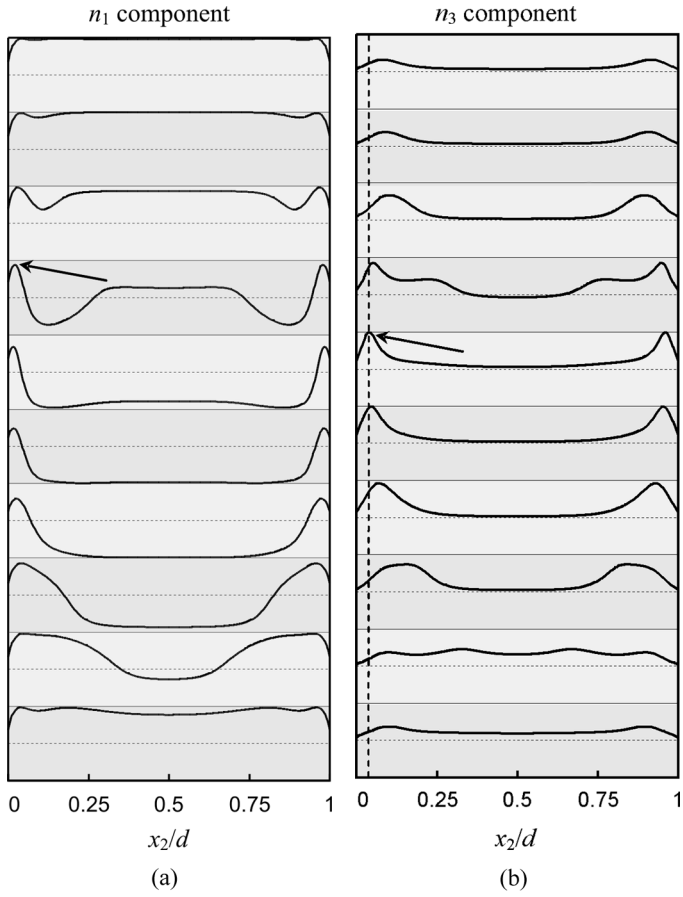

FIGURE 8 Director profiles for 8CB at different strains γ_i: from the top to the bottom we have $\gamma_i = i\gamma_0$ with $\gamma_0 = 1.87$ and $i \approx 20, 21, \ldots, 29$. Component n_1 in (a) and component n_3 in (b). The value of $9 \times \gamma_0$ corresponds approximately to a rotation by 2π of the director within the shear plane. These results have been obtained by solving Eqs. (7) and (8) with data of Tables 3 and 4. The dotted vertical line materialises the abscissa x_2^* defined in the text. The formation of the peaks for n_3 coincides with the unhook of n_1 from $+1$ as indicated by the arrows.

and then migrate towards the bulk. For fixed anchoring strength A_s there exists a shear rate $\dot{\gamma}_{\min}$ such that no oscillation occurs whatever $\vec{e}$ and $\dot{\gamma} \leq \dot{\gamma}_{\min}$; likewise, there exists a shear rate $\dot{\gamma}_{\max}$ such that no oscillation occurs whatever $\vec{e}$ and $\dot{\gamma} \geq \dot{\gamma}_{\max}$. For fixed easy axis $\vec{e}$ and anchoring strength A_s either no precession occurs whatever $\dot{\gamma}$ or

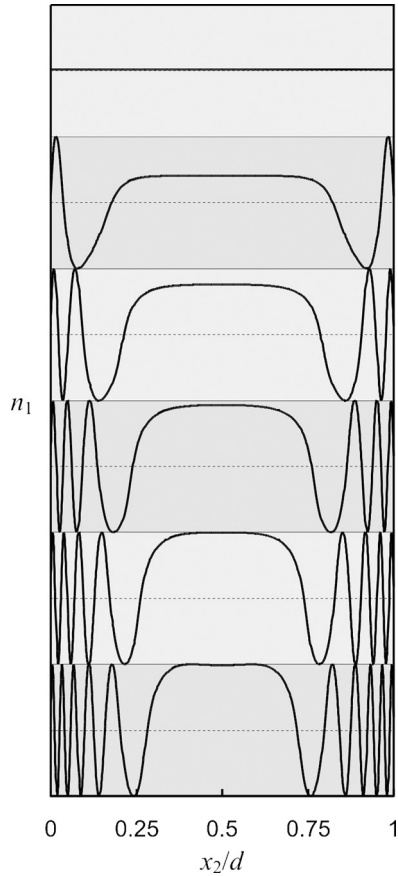

FIGURE 9 Profiles of the director component n_1 for 8CB when the director is constrained to stay within the shear plane at different strains γ_i: from the top to the bottom we have $\gamma_i = i\gamma_0$ with $\gamma_0 = 16.8$ and $i \approx 0, 1, \ldots, 5$; the value of γ_0 corresponds approximately to a rotation by 2π of the director within the shear plane. These results have been obtained by solving Eqs. (13*a*) and (14) with data of Tables 3 and 4 except for $A_s = 3.5 \times 10^{-5}\,\mathrm{J\,m^{-2}}$ (strong anchoring is necessary to evidence the director winding; for weak anchoring the distortion 'escapes through the boundaries').

TABLE 1 Model Parameters Used for Aligning Nematics

β_e (rd)	ψ_e (rd)	d (μm)	A_s ($\mathrm{J\,m^{-2}}$)
1.57	2.35	300	3.5×10^{-6}

TABLE 2 Material Parameters Used for Aligning Nematics. The Leslie Viscosities are those of MBBA at 20°C [7]. The Viscosities α_i ($i = 1, \ldots, 6$) are in Pa s and the Elastic Constant K is in Jm^{-1}

α_1	α_2	α_3	α_4	α_5	α_6	K
-2.15×10^{-2}	-1.53×10^{-2}	-7.70×10^{-4}	1.09×10^{-1}	1.07×10^{-1}	-4.71×10^{-2}	10^{-11}

precession occurs for $\dot{\gamma}_1 \leq \dot{\gamma} \leq \dot{\gamma}_2$ where $\dot{\gamma}_1$ and $\dot{\gamma}_2$ are function of $\vec{e}$ and A_s. For fixed shear rate $\dot{\gamma}$ and anchoring strength A_s allowing director precession, it effectively occurs for any $\vec{e}$ inside a solid angle. For the data in Tables 1 and 2 and $\dot{\gamma} = 15s^{-1}$ we get an oscillatory regime when $1.73 \pm 0.01\mathrm{rd} \leq \psi_e \leq 2.99 \pm 0.01\mathrm{rd}$ for $\beta_e = 1.57$ or when $0.65 \pm 0.01\mathrm{rd} \leq \beta_e \leq 2.51 \pm 0.01\mathrm{rd}$ for $\psi_e = 2.36$. When $\vec{e}$ lies in the vicinity of the centre of this solid angle, the amplitude of the director precession is strong; when, on the contrary, $\vec{e}$ approaches the edge of the solid angle the amplitude of the oscillation decreases.

It appears that neither homeotropic nor planar anchoring seems favourable for occurrence of precession which *a priori* makes difficult to observe this phenomenon experimentally because it requires to accurately control the easy axis. On the other hand, for the sake of simplicity the calculations presented here have been performed for the parallel plates geometry, which is not realistic since with this setup a constant shear rate cannot be carried out for a long time. Thus real experiments must be performed with Couette or cone-and-plate cell, which enhances the difficulty of imposing a controlled easy axis. In order to be allowed to use the results of this work for the interpretation of the experimental data it is required that locally the easy axis have the correct orientation with respect to the 'local characteristic directions' of the flow (i.e., velocity, velocity gradient and vorticity directions). That implies to impose an inhomogeneous easy axis field that satisfies the axial symmetry of the setup. This task is certainly hard. However, we would like to suggest that the 'anchoring gliding' phenomenon [9] might provide a practical means to control the easy axis. Indeed it has been observed that under torque the easy axis can rotate and can keep its new orientation after torque removal. This effect is assumed to result from adsorption/desorption process. In this work we have remarked that a convenient easy axis allowing pronounced director precession lies within the shear plane. Accordingly one may suggest to shear the sample strongly (with a shear rate that forbids any oscillatory regime) and for a long time in order to tilt the easy axis toward the velocity.

III-2 Tumbling Nematics

In this subsection we apply the equations of Section II to the tumbling system 8CB at 35°C. The model and material parameters are given in Tables 3 and 4 respectively.

Figures 6 to 8 show the profiles of the director component n_1 (Figs. 6a to 8a) and n_3 (Figs. 6b to 8b) at different equidistant times. They are obtained by solving Eqs. (7) and (8) with the data of Tables 3 and 4. In each figure the delay between the first profile and the last one corresponds approximately to a rotation by 2π of the director within the shear plane. For comparison, we show in Figure 9 the n_1 profile at different times when the director is constrained to stay within the shear plane, i.e., by solving Eqs. (13a) and (14) with the same parameters. In Figure 9 we can observe the increase with time of the number of oscillations in space of n_1 from -1 to $+1$; this feature actually reflects the winding of the director due to tumbling. On the contrary this feature is absent in Figures 6a to 8a when out of shear plane director is allowed, which indicates the absence of director winding in this case. On the other hand Figures 6b to 8b, showing n_3, evidence an interesting feature occurring in the vicinity of the bounding plates. Indeed, at (or close to) a position specified by the coordinate x_2^* and indicated by a vertical dotted line in Figures 6b to 8b, the director periodically comes out of the shear plane, reaches the vorticity axis ($n_3 = 1$, it is indicated by an arrow) and returns back close to the shear plane. When $n_3 = +1$ at x_2^* (and $d - x_2^*$ by symmetry) the n_3 profile exhibits two sharp peaks. The formation of these two peaks occurs when simultaneously the component n_1 seems to break some starting director winding. This latter remark is evidenced in Figures 6a to 8a by arrows that indicate the time at which the component n_1 unhooks from 1, as well as in Figs. 6b to 8b by arrows that indicate when $n_3 = 1$. In short, the director winding generated by tumbling is cancelled thanks to the periodic tilt of the director toward the vorticity at two symmetrical positions (x_2^* and $d - x_2^*$) close to the plates. It is worth noting that the position x_2^* varies only slightly from period to period and we have $x_2^* \approx 10\mu m$.

The degree of winding of the director around the vorticity axis, may be evaluated by the angle of rotation of the projection of the director within the shear plane when one follows the director in space from

TABLE 3 Model Parameters Used for Tumbling Nematics

β_e (rd)	ψ_e (rd)	d (μm)	A_s ($J\,m^{-2}$)	$\dot{\gamma}(s^{-1})$
1.55	1.55	400	3.5×10^{-6}	3

TABLE 4 Material Parameters Used for Tumbling Nematics. The Leslie Viscosities are those of 8CB at 35°C [7,10]. The Viscosities α_i (i = 1, . . . ,6) are in Pa s and the Elastic Constant K is in Jm^{-1}

α_1	α_2	α_3	α_4	α_5	α_6	K
1.34×10^{-3}	-6.90×10^{-2}	1.39×10^{-2}	5.60×10^{-2}	5.30×10^{-2}	-2.10×10^{-3}	10^{-11}

one bounding plate to the middle gap. Using the fact that the elementary angle of rotation $d\theta$ along an elementary path is given by

$$d\theta = \frac{n_2 dn_1 - n_1 dn_2}{n_1^2 + n_2^2} \tag{16}$$

where dn_1 and dn_2 denote the elementary variation of n_1 and n_2 along the same elementary path. The magnitude of the director rotation is obtained by integrating Eq. (16) over a line normal to the plate, starting on one plate and ending in the middle gap; we note $\Delta\theta$ this angle. Numerical application of Eq. (16) is difficult when n_3 becomes very close to one, for that reason we replaced Eq. (16) by

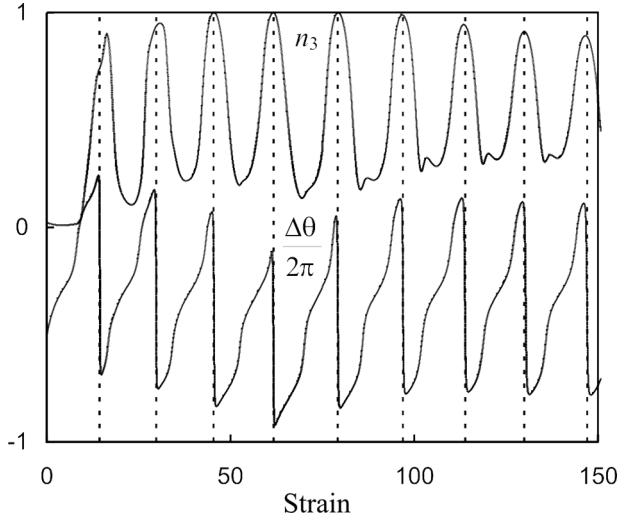

FIGURE 10 Strain dependence for 8CB of $n_3(x_2^*)$ for $x_2^* = 12.5\mu m$ and $\Delta\theta/2\pi$ where $\Delta\theta = \int_0^{d/2} (d\theta/dx_2)dx_2$ with $d\theta$ given by Eq. (17) and $\varepsilon = 10^{-3}$. These results have been obtained with data of Tables 3 and 4. For clarity the curve for $\Delta\theta/2\pi$ has been displaced along the ordinate axis. The sudden drops of $\Delta\theta$ coincide with $n_3(x_2^*) = 1$.

$$d\theta = \frac{n_2 dn_1 - n_1 dn_2}{n_1^2 + n_2^2 + \varepsilon} \tag{17}$$

with $0 < \varepsilon \ll 1$.

Figure 10 shows the strain dependence of $\Delta\theta/2\pi$ and $n_3(x_2^*)$, where x_2^* has been defined above, for the data of Tables 3 and 4. More precisely, the strain dependence of $n_3(x_2^*)$ has been obtained with $x_2^* = 12.5\mu$m. Figure 10 shows that $\Delta\theta$ is an oscillatory function of strain that periodically smoothly increases and suddenly drops to approximately its initial value, which confirms that the director does not wind permanently. The fact that $n_3(x_2^*)$ approaches 1 periodically illustrates what is shown by Figures 6b to 8b in a different manner. The main feature of Figure 10 is the clear coincidence in time of the sudden drop of $\Delta\theta$ with the maximum of $n_3(x_2^*)$. That enhances the previous conclusion according to which the unwinding of the director is performed through director tilt toward the vorticity axis at two positions at about 10 μm from the plates. Finally this behaviour allows the relaxation of the elastic free energy generated by the tumbling.

IV. CONCLUSION

This paper has been devoted to the director dynamics within boundary layers in nematic liquid crystals subjected to a simple shear flow and non-rigid anchoring. Leslie-Ericksen theory for nematodynamics and Rapini-Papoular model for anchoring provided the theoretical basis for this work. We have examined the cases of aligning and tumbling nematics. For aligning nematics we have found an oscillatory regime where the director undergoes a precession motion within the boundary layers while reaching a steady orientation in the bulk. This feature is specific to non-rigid anchoring and it arises when the easy axis and the shear rate take a limited range of values; in particular, the easy axis needs to be tilted from homeotropic orientation toward the velocity. Concerning tumbling nematics, we have evidenced a mechanism of relaxation of the elastic energy accumulated during the shearing and resulting from director winding. Some unwinding of the director is allowed by periodic and local out-of-plane director motion in the vicinity of the bounding plates; more precisely, at a particular position, about 10 μm from the plates, the director drifts toward the vorticity axis and exactly reaches this orientation before returning back close to the shear plane. We conclude from this study that when the director is free to explore the three dimensions of space the elastic distortion induced by flow relaxes quite easily so that elastic forces stay relatively weak.

REFERENCES

[1] Leslie, F. M. (1968). *Arch. Rat. Mech. Anal.*, *28*, 265.
[2] de Gennes, P. G., *et al.* (1993). *The physics of liquid crystals*, 2nd ed., Oxford University Press: Oxford.
[3] Rapini, A. & Papoular, M. (1969). *J. Phys.*, *30C*, 4.
[4] Mikhlin, S. G. (1970). *Mathematical physics, an advanced course*. North-Holland series in Applied mathematics and mechanics, North-Holland publishing company: Amsterdam.
[5] Fletcher, C. A. J. (1991). *Computational Techniques for fluid dynamics*. 2nd ed., Springer Series in Computational Physics, Springer-Verlag: Heidelberg.
[6] Blinov, L. M., Kabayenkov, A. Yu., & Sonin, A. A. (1989). *Liq. Cryst.*, *5*, 645.
[7] Kneppe, H., Schneider, F., & Sharma, N. K. (1981). *Ber. Bunsenges. Phys. Chem.*, *85*, 784; Kneppe, H., Schneider, F., & Sharma, N. K. (1982). *J. Chem. Phys.*, *77*, 3203.
[8] Karat, P. P. & Madhusudana, N. V. (1977). *Mol. Cryst. Liq. Cryst.*, *40*, 239.
[9] Stoenescu, D. N., Dozov, I., Martinot-Lagarde, P. (2001). *Mol. Cryst. Liq. Cryst.*, *351*, 427.
[10] Gu, D.-F., Jamieson, A. M., & Wang, S.-Q. (1993). *J. Rheol.*, *37*, 985.